EDDY WIJANTO-FILE 5

by Eddy Wijanto-file 5 Eddy Wijanto-file 5

Submission date: 14-Feb-2023 02:09PM (UTC+0700)
Submission ID: 2013876970
File name: IEEE_Access_Journal.pdf (5.19M)
Word count: 6511
Character count: 32513

IEEE Access
Multidisciplinary | Rapid Review | Open Access Journal

Received March 11, 2020, accepted April 1, 2020, date of publication April 28, 2020, date of current version May 15, 2020.

Digital Object Identifier 10.1109/ACCESS.2020.2991071

Multiple Access Techniques for Bipolar Optical Code Division in Wireless Optical Communications

HSU-CHIH CHENG[1], EDDY WIJANTO[1], TZU-CHIEH LIEN[1], PO-HAN LAI[1], AND SHIN-PIN TSENG[2]

[1]Department of Electro-Optical Engineering, National Formosa University, Yunlin 632, Taiwan
[2]Department of Electronic Engineering, National United University, Miaoli 36003, Taiwan

Corresponding author: Shin-Pin Tseng (sptseng@nuu.edu.tw)

This work was supported by the Ministry of Science and Technology, Taiwan, under Grant MOST 108-2221-E-150-041 and Grant MOST 108-2221-E-239-003.

ABSTRACT In this paper, multiple access techniques for bipolar optical code division are proposed for application in wireless optical communications. First, several fiber Bragg gratings (FBGs) and optical circulators are used to encode optical signals. Then, the horizontal or vertical polarization state can be controlled using bipolar data. Experiments were conducted using two devices to determine the feasibility of using multiple access techniques for bipolar optical code division in free-space optical communication. The first experiment tested the first architecture, in which each user operates a mechanical optical switch by switching data bits to generate optical signals with specific polarization states through a collimator in a free-space channel. As the decoding components, several FBGs and optical circulators are used as primary devices. Decoded signals are sent to a balanced photodetector, which can reconstruct original data from the encoder. The second experiment involved a second architecture, in which an encoder with an erbium-doped fiber amplifier and a decoder with an attenuator are used to improve system stability. The third experiment was designed to test whether multiple access interference can be alleviated with the proposed architectures. In the final experiment, an ultrafast optical switch was used instead of the original optical switch for selecting optical signals with a specific polarization state to improve the overall transmission rate. The experimental results indicate that the proposed scheme could be successfully implemented in free-space optical communication systems. The architectures of the proposed scheme mitigate multiple access interference with a simple and cost-effective design.

INDEX TERMS Bipolar, free-space optical communication, multiple access interference, optical code-division multiple access.

I. INTRODUCTION

Because of the limitations of wired optical networks, such as the inability to satisfy requirements for application in certain environments, wireless optical communication (WOC) networks have become an important research topic in recent years. However, wireless communication also has certain limitations. Wireless communication is strictly regulated in particular scenarios, such as communication between airport towers and aircraft. Furthermore, precision instruments used in clinical settings are subject to electromagnetic wave interference (EMI). The development of WOC systems is crucial for solving real-world problems. However, to develop such systems, some problems must be overcome in free-space optical (FSO) communication. For example, long-distance transmission involves considerable power attenuation, and outdoor wireless transmission is susceptible to influenced by atmospheric and environmental conditions (e.g., rain and fog).

Research on multiplex processing in FSO communication systems is crucial. The first multiplex processing scheme originated from time-division multiplexing techniques [1]. According to its operating principle, input signals are multiplexed into different time slots. One advantage of multiplex

The associate editor coordinating the review of this manuscript and approving it for publication was Tariq Umer.

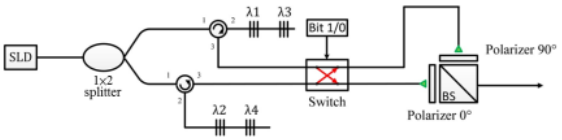

FIGURE 1. Proposed bipolar OCDMA encoder.

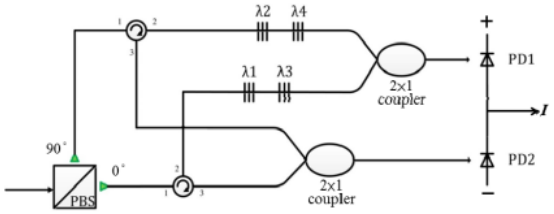

FIGURE 2. Design of the proposed bipolar OCDMA decoder.

processing is that it allows all users to optical signals at the same wavelength. However, adjacent wavelengths still require a time delay for accessing the correct wavelength signal. Thus, if the number of users is large, a long fiber must be used. Another multiplex technique, which is termed wavelength-division multiplexing, involves using multiple wavelengths as the transmission signals of multiple users. However, in this approach, the number of users is limited by the light-source bandwidth [2], [3].

Many researchers have used the novel multiplexing technique of optical code-division multiple access (OCDMA) [4], [5]. In this approach, code-division multiple access is applied for optical fiber communication. Thus, in OCDMA communication systems, an optical coding technique is employed in which each user is assigned a codeword to avoid mutual interference in the same channel. This technique enables the simultaneous transmission of unsynchronized data from multiple users of the same channel and bandwidth [6]. The multiplex technique provides favorable antijamming properties, a moderate security level, and high-capacity processing. Spectral amplitude coding (SAC) is an attractive OCDMA scheme because of its ability to mitigate multiple access interference (MAI) [5].

For the demodulation of optical signals, OCDMA schemes can be divided into coherent and incoherent schemes. Incoherent OCDMA schemes harness optical field intensity for encoding optical signals. The main encoding method used is unipolar encoding (0, 1). Unipolar encoding architectures have simple and low-cost designs; however, the number of codes that can be provided to users is considerably smaller in unipolar encoding architectures than in bipolar encoding architectures. An increase in the number of users necessitates an increase in code length. Coherent systems function by encoding the input light phase through a matching filter to change the phase of the optical signal [7].

In 2007, Zeng *et al.* [8] proposed a unipolar encoding/bipolar decoding OCDMA scheme. They employed an electro-optic phase modulator and two fiber Bragg gratings (FBGs) to construct a sequence-inversion-keyed system. This system has low complexity because each unipolar encoder or decoder uses only two FBG array. However, the corresponding bipolar decoders are implemented using a series of FBGs, which limits the decoding process and system transmission rate.

In 2006, Chang and Huang [9] designed a spectral polarization coding scheme for an OCDMA network. A corresponding codec is established using several FBGs and polarization beam splitters. This coding scheme is employed to modulate the wavelengths of an optical signal with unique polarization components. The results of Chang *et al.* indicated that MAI could be reduced using the aforementioned scheme, which is consistent with the results obtained in previous studies using SAC schemes. However, the polarization state of the optical signal in this system is unstable during long-distance fiber transmission. Moreover, the complexity of its codec is high.

In this paper, a novel bipolar scheme is presented. A Walsh–Hadamard (WH) code was used to construct the scheme. Then, a simple architecture was developed using WH codes and several FBGs. The system is simple and provides advantages such as a straightforward design, low cost, and moderate security level. Because the proposed approach involves using an FSO communication technique to eliminate the necessity of using a star coupler, the topology is suitable for application in mountain-to-mountain communication. We conducted four experiments to verify the feasibility of the proposed system. The first experiment was performed to determine whether the proposed bipolar scheme functions properly. Certain atmospheric parameters can attenuate the intensity of optical signals transmitted in free space and were measured. In the second experiment, an erbium-doped fiber amplifier (EDFA) was used as a preamplifier for the encoder. Moreover, an attenuator was employed in the decoder to compensate for the different power levels of the components. In the third experiment, the another decoder was tested to determine if MAI could be completely eliminated with the proposed scheme. From the first experimental results, the limitation of the switch caused performance degradation during decoding. Therefore, in the final experiment, an ultrafast optical switch was used to improve the system performance.

The remainder of this paper is organized as follows. Section II describes the proposed bipolar OCDMA scheme and the corresponding system design. Section III presents the experimental results for FSO communication systems using bipolar OCDMA schemes, such as systems using a mismatched decoding process, and describes the system stability improvements achieved using an attenuator and EDFA. Finally, the conclusions are provided in Section IV.

II. PROPOSED BIPOLAR OCDMA TECHNIQUE

The proposed bipolar OCDMA technique is used to transmit bipolar data signals, and the optical signals of each user are transmitted over a common FSO path. In the proposed system

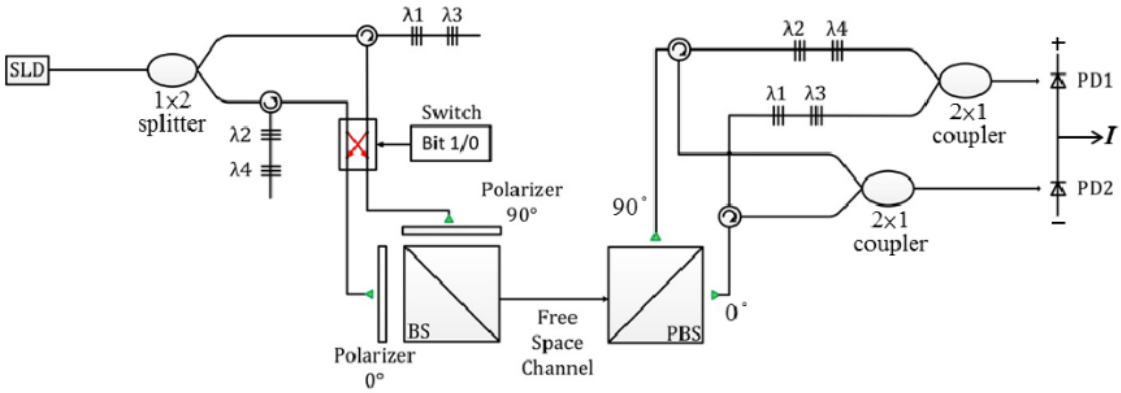

FIGURE 3. FSO communication system using bipolar OCDMA schemes.

design, FBGs are used as encoder and decoder devices. For data processing, an optical switch is used to encode the data bit of each user into an optical signal, which is transmitted to the decoder end through an FSO channel.

A WH code is used in the FSO OCDMA communication system because of its orthogonality. The WH matrix design is adopted from the matrix design in [8].

$$\boldsymbol{H}_1 = \begin{bmatrix} 1 & 1 \\ 1 & -1 \end{bmatrix} \quad \text{and } \boldsymbol{H}_n = \begin{bmatrix} \boldsymbol{H}_{n-1} & \boldsymbol{H}_{n-1} \\ \boldsymbol{H}_{n-1} & -\boldsymbol{H}_{n-1} \end{bmatrix}, \quad n = 2, 3, 4, \ldots, \tag{1}$$

where N is equal to 2^n and denotes the length of the WH code and the kth row of the matrix represents the kth optical codeword of the WH code assigned to the kth user. For example, when $N = 4$, the matrix of the proposed WH code can be expressed as follows:

$$\boldsymbol{H}_2 = \begin{bmatrix} 1 & 1 & 1 & 1 \\ 1 & -1 & 1 & -1 \\ 1 & 1 & -1 & -1 \\ 1 & -1 & -1 & 1 \end{bmatrix} = \begin{bmatrix} 1 & 1 & 1 & 1 \\ 1 & 0 & 1 & 0 \\ 1 & 1 & 0 & 0 \\ 1 & 0 & 0 & 1 \end{bmatrix} - \begin{bmatrix} 0 & 0 & 0 & 0 \\ 0 & 1 & 0 & 1 \\ 0 & 0 & 1 & 1 \\ 0 & 1 & 1 & 0 \end{bmatrix} = \boldsymbol{C}_{\mathrm{V}} - \overline{\boldsymbol{C}}_{\mathrm{H}}. \tag{2}$$

In (2), $\boldsymbol{h}_k$ denotes the kth row in the WH matrix to be decomposed into two unipolar codes, namely $\boldsymbol{c}_{k\mathrm{V}}$ and $\overline{\boldsymbol{c}}_{k\mathrm{H}}$. The codes $\boldsymbol{c}_{k\mathrm{V}}$ and $\overline{\boldsymbol{c}}_{k\mathrm{H}}$ represent the positive and negative elements of $\boldsymbol{h}_k$, respectively, and form a complementary pair in the set $\in \{0, 1\}$. With the above approach, $\boldsymbol{h}_k$ is transmitted for a data bit "1" for the kth user, whereas the complement row of $\boldsymbol{h}_k$ ($\overline{\boldsymbol{h}}_k$) is transmitted for a data bit "0" of the kth user. The notation $(\boldsymbol{C}_{\mathrm{V}} - \overline{\boldsymbol{C}}_{\mathrm{H}})$ represents the matrix formed when all users send a data bit "1." The WH matrix can be mapped to the wavelength domain and characterized by one of two orthogonal polarization states: vertical or horizontal. In the second equality of (2), the first and second matrices are assigned to the vertical ($\boldsymbol{C}_{\mathrm{V}}$) and horizontal ($\overline{\boldsymbol{C}}_{\mathrm{H}}$) polarization states, respectively. Similarly, the complement matrix of $\boldsymbol{H}_2$ can be decomposed as follows:

$$\overline{\boldsymbol{H}}_2 = \begin{bmatrix} -1 & -1 & -1 & -1 \\ -1 & 1 & -1 & 1 \\ -1 & -1 & 1 & 1 \\ -1 & 1 & 1 & -1 \end{bmatrix} = \begin{bmatrix} 0 & 0 & 0 & 0 \\ 0 & 1 & 0 & 1 \\ 0 & 0 & 1 & 1 \\ 0 & 1 & 1 & 0 \end{bmatrix} - \begin{bmatrix} 1 & 1 & 1 & 1 \\ 1 & 0 & 1 & 0 \\ 1 & 1 & 0 & 0 \\ 1 & 0 & 0 & 1 \end{bmatrix} = \overline{\boldsymbol{C}}_{\mathrm{V}} - \boldsymbol{C}_{\mathrm{H}}. \tag{3}$$

Therefore, the optical codeword $\boldsymbol{R}_k$, which is sent from the encoder of the kth user, can be expressed as follows:

$$\boldsymbol{R}_k = (\boldsymbol{c}_{k\mathrm{V}} - \overline{\boldsymbol{c}}_{k\mathrm{H}}) + (1 - b_k)\,(\overline{\boldsymbol{c}}_{k\mathrm{V}} - \boldsymbol{c}_{k\mathrm{H}})\,, \tag{4}$$

where $b_k \in \{0,1\}$ and $\boldsymbol{c}_{k\mathrm{V}}$ and $\boldsymbol{c}_{k\mathrm{H}}$ are the kth code encoded in the vertical and horizontal polarization states, respectively. Thus, if $b_k = 1$, the spectrum of the coded signal corresponds to $(\boldsymbol{c}_{k\mathrm{V}} - \overline{\boldsymbol{c}}_{k\mathrm{H}})$. Similarly, if $b_k = 0$, the spectrum of the coded signal is $(\overline{\boldsymbol{c}}_{k\mathrm{V}} - \boldsymbol{c}_{k\mathrm{H}})$. To apply WH codes with length N in the proposed schemes, the results of the following equations must be obtained:

$$\theta_{hh}(k, l) = \sum_{i=1}^{N} (\boldsymbol{c}_{k\mathrm{V}}(i) - \overline{\boldsymbol{c}}_{k\mathrm{H}}(i))\,(\boldsymbol{c}_{l\mathrm{V}}(i) - \overline{\boldsymbol{c}}_{l\mathrm{H}}(i)) = \begin{cases} N, & k = l \\ N/2, & k \neq l \end{cases} \tag{5}$$

and

$$\theta_{h\overline{h}}(k, l) = \sum_{i=1}^{N} (\boldsymbol{c}_{k\mathrm{V}}(i) - \overline{\boldsymbol{c}}_{k\mathrm{H}}(i))\,(\overline{\boldsymbol{c}}_{l\mathrm{V}}(i) - \boldsymbol{c}_{l\mathrm{H}}(i)) = \begin{cases} 0, & k = l \\ N/2, & k \neq l. \end{cases} \tag{6}$$

With the results of (5) and (6), the WH codes can be implemented in an FSO OCDMA communication system to mitigate MAI by using mathematical subtraction.

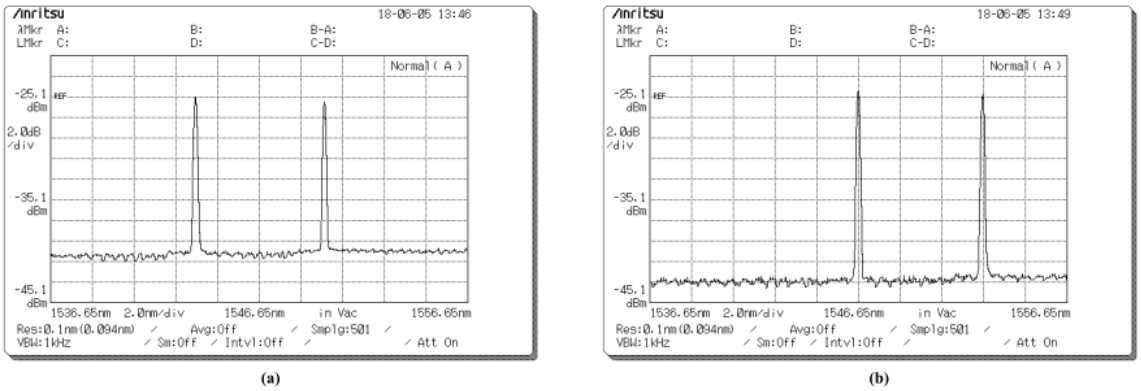

FIGURE 4. Reflected spectra used for (a) user 2 (λ_1 and λ_3) and (b) user 2 (λ_2 and λ_4).

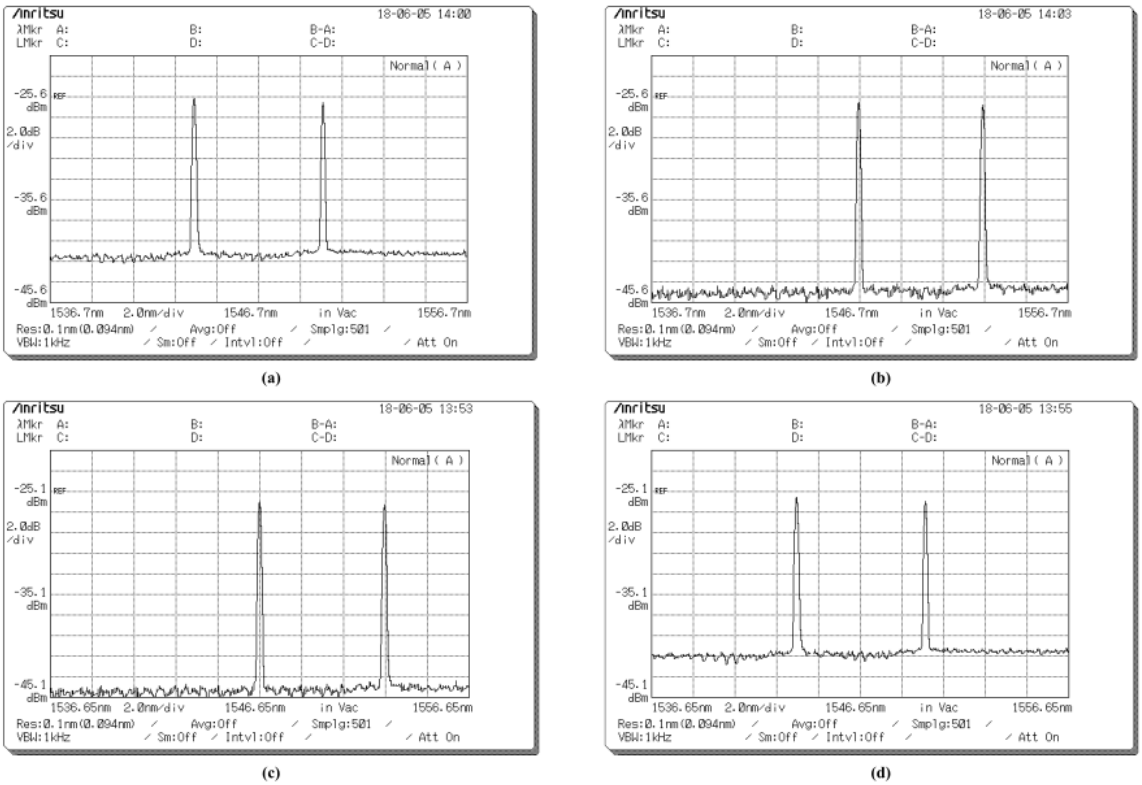

FIGURE 5. Output spectra at the output ports of the MEMS fiber optical switch operating with different data bits. (a) Optical spectra output from port 1 in the optical switch for a data bit "1." (b) Optical spectra output from port 1 in the optical switch for a data bit "0." (c) Optical spectra output from port 2 in the optical switch for a data bit "1." (d) Optical spectra output from port 2 in the optical switch for a data bit "0."

Through the aforementioned derivations, an FSO communication system can be constructed using bipolar OCDMA schemes. Fig. 1 displays the design of the proposed encoder with a WH code length of 4. It includes a superluminescent diode (SLD) light source, a 1 × 2 splitter, two optical circulators, two series of FBGs, a polarization beam splitter (PBS), and a 2 × 2 optical switch for selecting optical signals with the appropriate polarization components.

First, the optical signal of the SLD output is input to two optical circulators through the 1 × 2 splitter. Then, the two

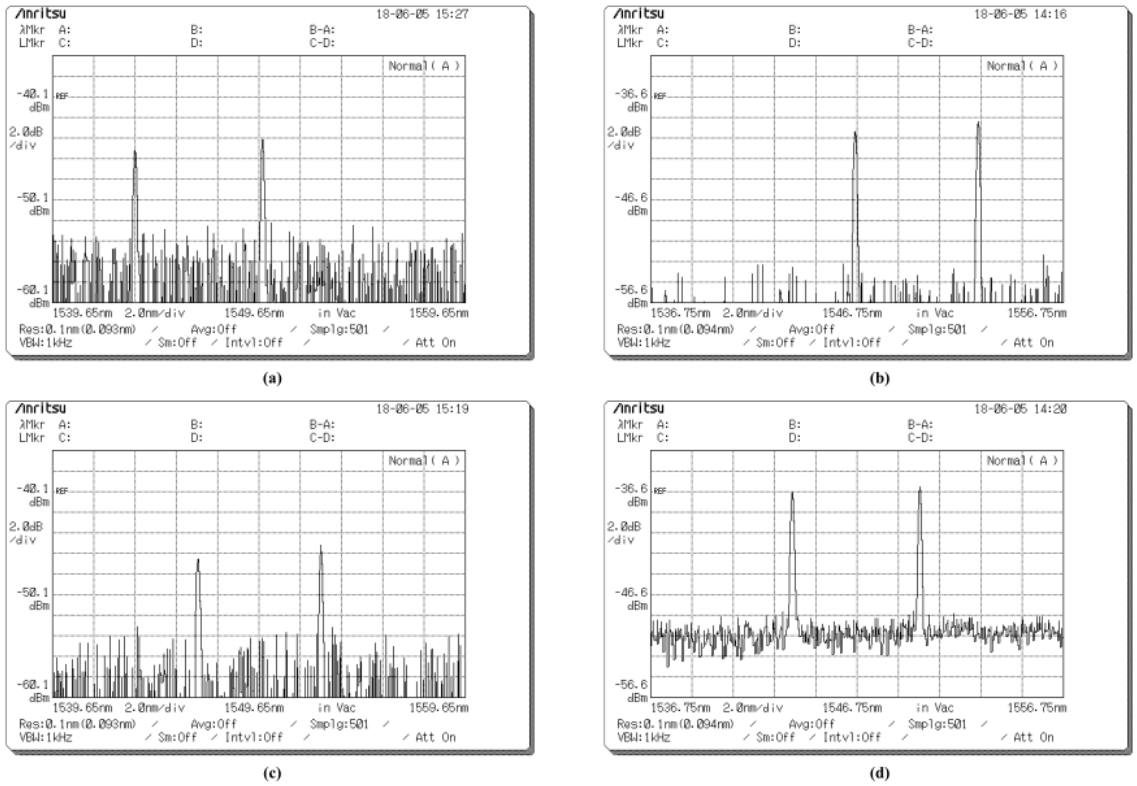

FIGURE 6. Output spectra at the output ports of the PBS in Decoder 2 for different data bits. (a) Optical spectra from output port 1 in the PBS for data bit "1." (b) Optical spectra from output port 2 in the PBS for data bit "1." (c) Optical spectra from output port 1 in the PBS for data bit "0." (d) Optical spectra from output port 2 in the PBS for data bit "0." .

ports of two optical circulators are connected to two series of FBGs according to the assigned optical codewords derived from the WH code ($\boldsymbol{h}_k$). For example, when $N = 4$, the encoder of the second user uses a series of upper FBGs to reflect the optical signals with wavelengths λ_1 and λ_3, which are transmitted to the first input port of the 2×2 optical switch through the circulator. Similarly, the optical signals with wavelengths λ_2 and λ_4 are transmitted to the second input port of the 2×2 optical switch. Then, the bipolar OCDMA scheme can be implemented using an optical switch according to the data bit of each user. If the data bit of the user is "1," the input signals pass parallel to each other into the PBS. Conversely, when the data bit of the user is "0," the input optical signals cross each other to pass through the optical switch before arriving at the input ports of the PBS. Therefore, optical signals with appropriate wavelengths and polarization states arrive at the output port of the PBS. Finally, the signals at the output port of each encoder are coupled to a fiber collimator and then transmitted into free space to implement the FSO communication system.

The design of the proposed decoder is illustrated in Fig. 2. The decoder comprises a PBS, two optical circulators, two series of FBGs, two 2×1 couplers, and a balanced photodetector (BPD) for mitigating the influence of MAI. First, the received FSO signal is input into a fiber collimator before being converted into an optical signal. Subsequently, the optical signal ($\boldsymbol{R}$) from the output port of the fiber collimator is depolarized into two optical circulators through the PBS. Therefore, the vertical polarization (90°) component of the incident signals appears only at the first port of the upper optical circulator, whereas the horizontal polarization (0°) component of the incident signals appears only at the first port of the lower optical circulator.

Let the intensity of the received optical signal ($\boldsymbol{R}$) be proportional to $\boldsymbol{R}_{\mathrm{V}} + \boldsymbol{R}_{\mathrm{H}}$.

$$\begin{aligned} \boldsymbol{R}_V &= \sum_{k=1}^{K} b_k \boldsymbol{c}_{k\mathrm{V}} + (1 - b_k)\, \bar{\boldsymbol{c}}_{k\mathrm{V}} \quad \text{and } \boldsymbol{R}_{\mathrm{H}} \\ &= \sum_{k=1}^{K} b_k \bar{\boldsymbol{c}}_{k\mathrm{H}} + (1 - b_k)\, \boldsymbol{c}_{k\mathrm{H}}, \end{aligned} \tag{7}$$

where K is the number of active users, $\boldsymbol{R}_{\mathrm{V}}$ is the sum of the intensities of the optical signals with only vertical polarization components, and $\boldsymbol{R}_{\mathrm{H}}$ is the sum of the intensities of the optical signals with only horizontal polarization components.

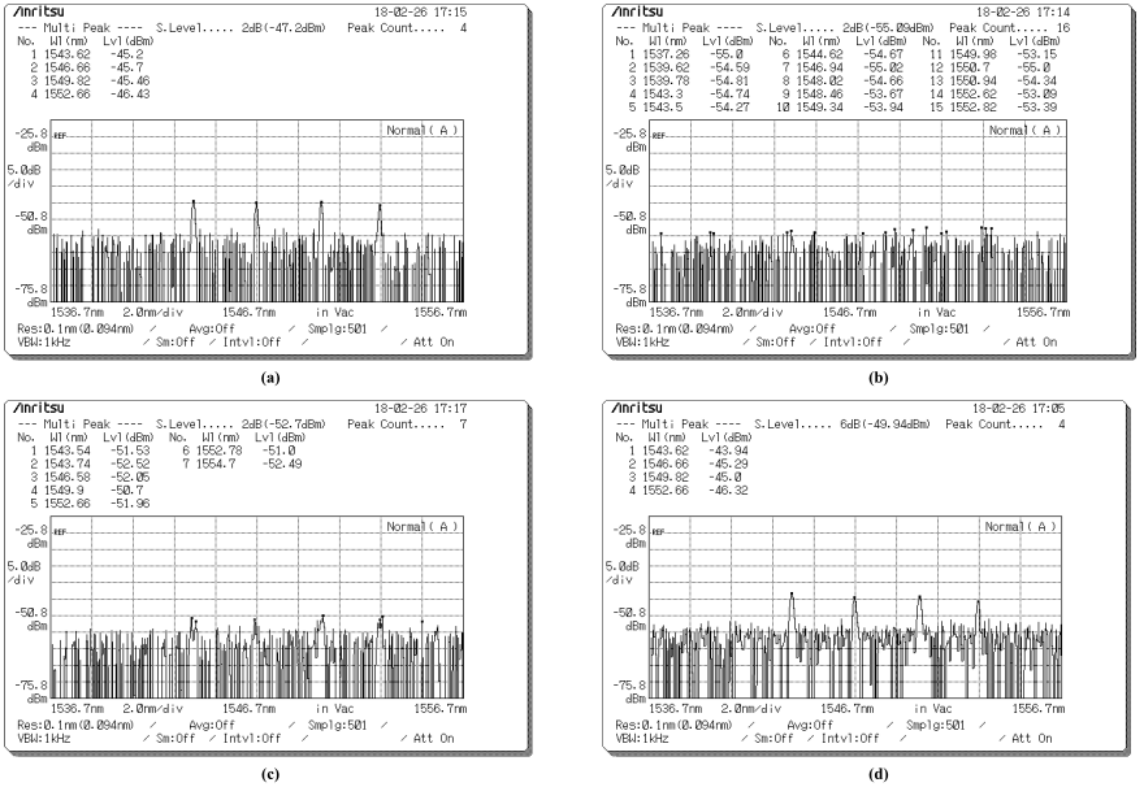

FIGURE 7. Decoded spectra at the output ports of the optical couplers at different data bits. (a) Optical spectra at the output port of the upper coupler in Decoder 2 for sending data bit "1." (b) Optical spectra at the output port of the lower coupler in Decoder 2 for sending data bit "1." (c) Optical spectra at the output port of the upper coupler in Decoder 2 for sending data bit "0." (d) Optical spectra at the output port of the lower coupler in Decoder 2 for sending data bit "0."

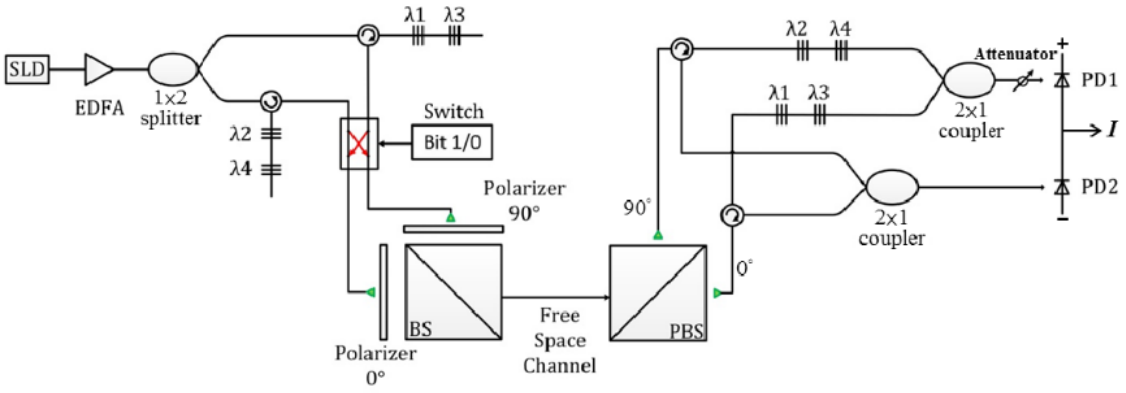

FIGURE 8. Proposed bipolar OCDMA–FSO communication system involving the use of an EDFA and attenuator.

According to (7), the optical signals ($\boldsymbol{R}_{\mathrm{V}}$) with wavelengths corresponding to the "1s" position of $\overline{\boldsymbol{c}}_{k\mathrm{V}}$ are reflected by a series of FBGs in the decoder for the kth user. These reflected signals then arrive at the first input port of the lower 2 × 1 coupler. Simultaneously, the optical signals ($\boldsymbol{R}_{\mathrm{V}}$) with residual wavelengths corresponding to the "1s" position of $\boldsymbol{c}_{k\mathrm{V}}$ are transmitted to the first input port of the upper 2 × 1 coupler. Similarly, the optical signals ($\boldsymbol{R}_{\mathrm{H}}$) with wavelengths corresponding to the position of the "1s" of $\boldsymbol{c}_{k\mathrm{H}}$ arrive at the second input port of the upper 2 × 1 coupler after being

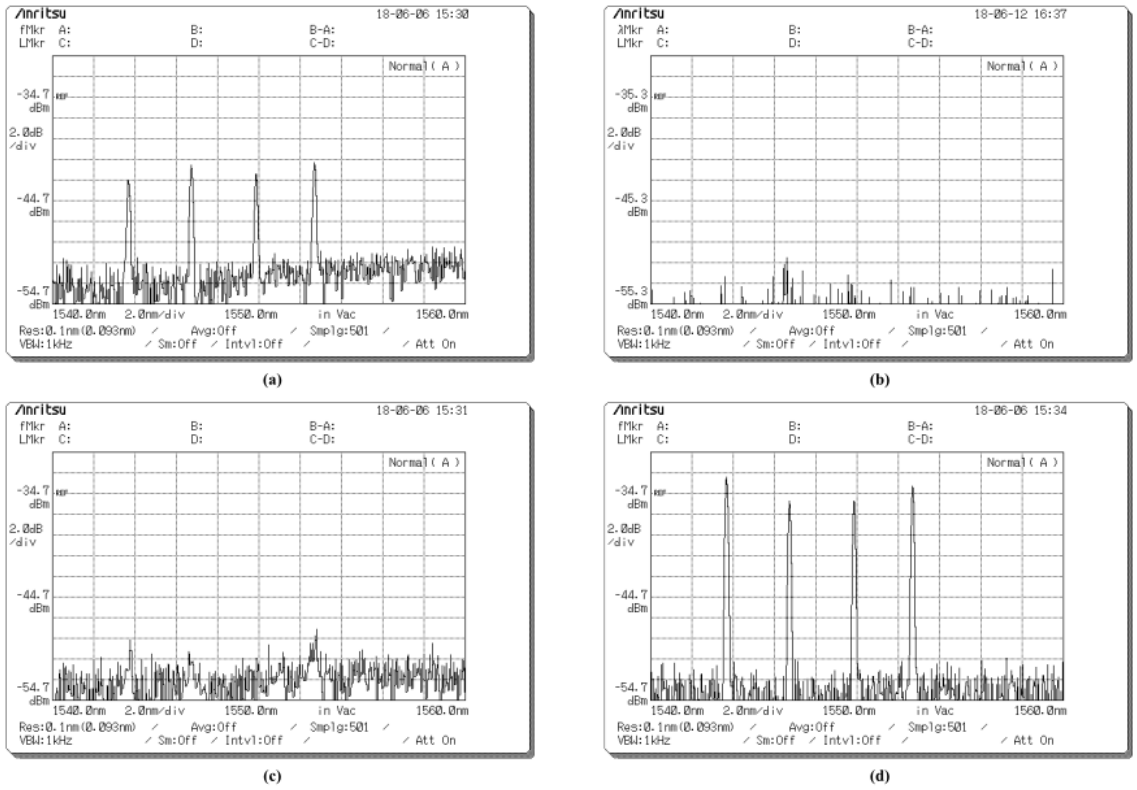

FIGURE 9. Decoded spectra at the output ports of the attenuator and the lower coupler at different data bits. (a) Optical spectra at the output port of the attenuator in decoder 2 for sending data bit "1." (b) Optical spectra at the output port of the lower coupler in decoder 2 for sending data bit "1." (c) Optical spectra at the output port of the attenuator in decoder 2 for sending data bit "0." (d) Optical spectra at the output port of the lower coupler in decoder 2 for sending data bit "0."

reflected by a series of lower FBGs. Concurrently, the optical signals ($\boldsymbol{R}_{\mathrm{H}}$) with reflected wavelengths are transmitted to the second input port of the lower 2×1 coupler. Then, the optical signals at the output ports of the upper and lower 2×1 coupler are transmitted to the input ports of the BPD to respectively conduct correlation subtraction and eliminate MAI. The aforementioned approach is detailed in the following equation.

$$\theta_{xh}(k,l) - \theta_{x\overline{h}}(k,l) = \begin{cases} N, & \text{if } x = h, k = l \\ -N, & \text{if } x = \overline{h}, k = l \\ 0, & \text{otherwise,} \end{cases} \tag{8}$$

where $\boldsymbol{h}_l$ and $\overline{\boldsymbol{h}}_l$ denote the assigned and complementary optical codewords of the desired user. Finally, the decision current (I) is used to determine the data bit of the desired user in the FSO channel.

III. EXPERIMENTAL SETUP AND RESULTS

The objective of the experiments was to test the feasibility of FSO communication systems using the proposed bipolar OCDMA schemes. The experimental FSO communication system using WH codes with $N = 4$ is displayed in Fig. 3. The NXTAR SLD-2000 was adopted as an SLD light source with stable power. Furthermore, wideband couplers (Fiber Optic Communications, Inc., Taiwan) were used as 2×1 couplers and the 1×2 splitter. An Anritsu MS9170C optical spectrum analyzer was used to determine the accuracy of the spectral codec output. The BPD model used for decoding was Model 1817 (New Focus Inc., CA, USA), which was used to perform signal subtraction in the optical domain and then convert the results into electrical signals. A ±15-V current-limited power supply was used to power the BPD. Moreover, a Tektronix TDS2102B digital oscilloscope was used for monitoring the signal output of the BPD. Finally, a Twintx TFG 3510 signal generator was used to obtain square waves with different duty cycles to simulate the data transmission by multiple users.

The FBG resonance wavelengths used for the FBG codecs used in this study were 1543, 1546, 1549, and 1552 nm, represented by $\lambda_1, \lambda_2, \lambda_3$, and λ_4, respectively. The aforementioned wavelengths correspond to the binary sequences of −1s and 1s. We made the following preliminary assumptions: (1) The WH codes ($\boldsymbol{h}$) for the four users are $\boldsymbol{h}_1 = (1, 1, 1, 1)$,

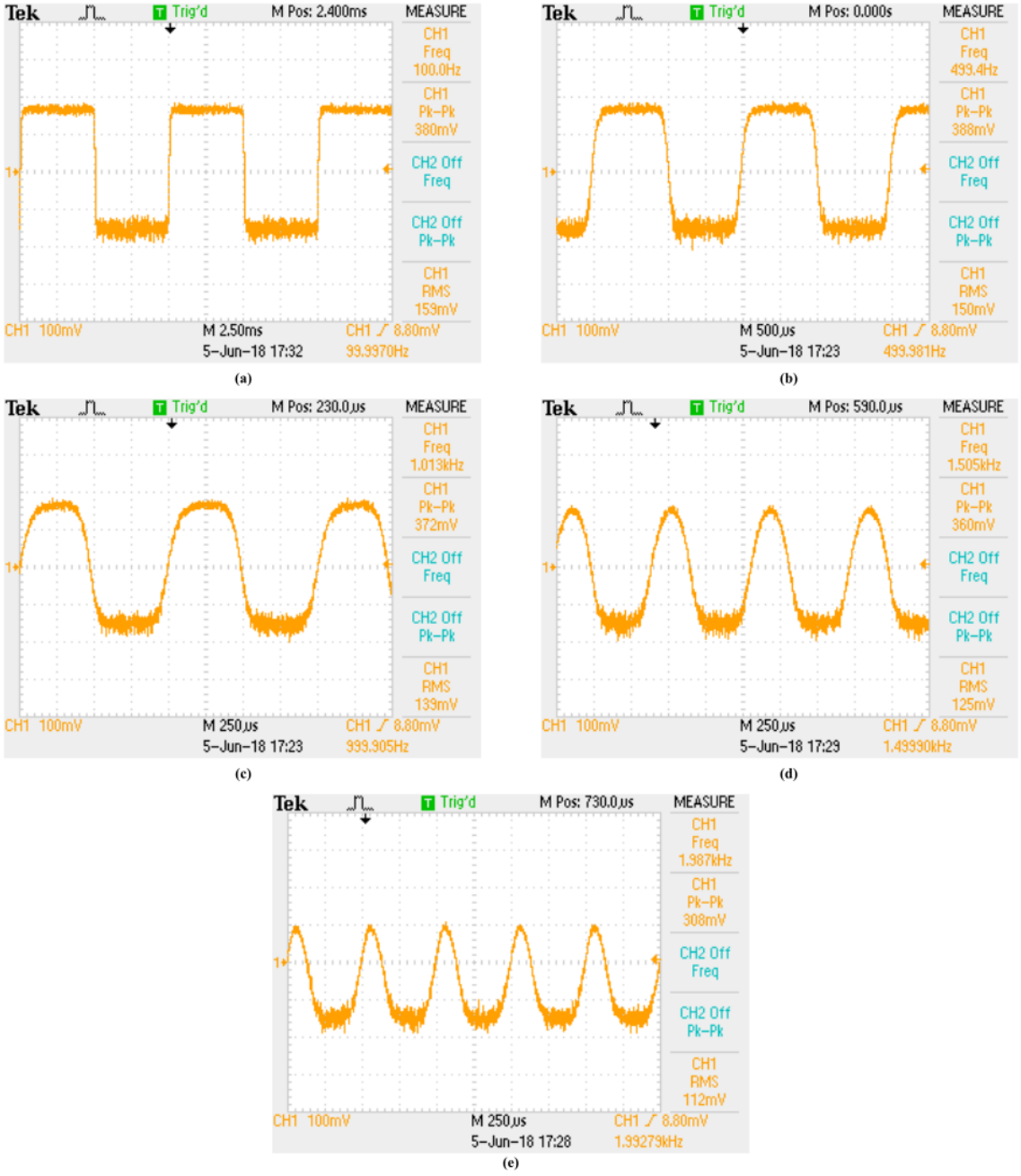

FIGURE 10. Decoding results for Decoder 2 with input signal frequencies of (a) 0.1, (b) 0.5, (c) 1, (d) 1.5, and (e) 2 kHz for Encoder 2.

$\boldsymbol{h}_2 = (1, -1, 1, -1)$, $\boldsymbol{h}_3 = (1, 1, -1, -1)$, and $\boldsymbol{h}_4 = (1, -1, -1, 1)$. (2) The corresponding binary sequence for $\boldsymbol{h}_1$ is 1s when the encoding wavelengths for the first user are λ_1, λ_2, λ_3, and λ_4 for vertical polarization. (3) The binary sequence for $\boldsymbol{h}_2$ is 1s when the encoding wavelengths for the second user are λ_1 and λ_3 for vertical polarization and λ_2 and λ_4 for horizontal polarization. (4) The binary sequence for $\boldsymbol{h}_3$ is 1s when the encoding wavelengths for the third user are λ_1 and λ_2 for vertical polarization and λ_3 and λ_4 for horizontal polarization. (5) The binary sequence for $\boldsymbol{h}_4$ is 1s when the

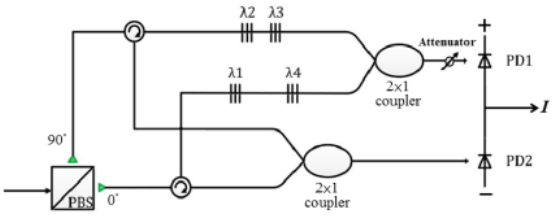

FIGURE 11. Block diagram of FBG decoder 4.

encoding wavelengths for the fourth user are λ_1 and λ_4 for vertical polarization and λ_2 and λ_3 for horizontal polarization. In the experiments, only the WH codes of users 2 and 4 were used to design the FBG codec. An OSW22-1310E MEMS fiber optical switch kit (Thorlabs, NJ, USA) was used as the 2×2 optical switch in the first experiment.

Fig. 4(a) and (b) displays the measured reflected spectra [(λ_1, λ_3) and (λ_2, λ_4), respectively] for user 2, which are represented as $(1, -1, 1, -1)$. At port 3 of the upper optical circulator of encoder 2, the central wavelengths of λ_1 and λ_3 were 1543 and 1549 nm, respectively, and the corresponding light intensities were −25.1 and −25.51 dBm, respectively. Moreover, at port of the lower optical circulator of encoder 2, the central wavelengths of λ_2 and λ_4 were 1546 and 1552 nm, respectively, and the corresponding light intensities were −24.46 and −24.78 dBm.

Fig. 5 displays the outputs of the MEMS fiber optical switch operating with different data bits in encoder 2. Fig. 5(a) illustrates the output spectrum from the first output port of the optical switch when the data bit of user 2 was "1." In this condition, the central wavelengths at the port were 1543 and 1549 nm, with light intensities of −25.68 and −26.1 dBm, respectively. Fig. 5(b) illustrates the output spectrum from the first output port of the optical switch when the data bit of user 2 was "0." In this condition, the central wavelengths at the port were 1546 and 1552 nm, with light intensities of −26.08 and −26.94 dBm, respectively. Fig. 5(c) illustrates the output spectrum from the second output port of the optical switch when the data bit of user 2 was "1." In this situation, the central wavelengths at the port were 1546 and 1552 nm, with light intensities of −26.04 and −26.21 dBm, respectively. Fig. 5(d) depicts the output spectrum from the first output port of the optical switch when the data bit of user 2 was "0." In this situation, the central wavelengths at the port were 1543 and 1549 nm, with light intensities of −25.59 and −26 dBm, respectively. A comparison of Figs. 4 and 5 reveals that the light intensity output by the optical switch lost approximately 1 dB for the reflected spectra.

After propagation through the PBS into a free-space channel, the encoded spectra with specific polarization states from FBG encoder 2 were sent to FBG decoder 2 for decoding. The received optical signals were then depolarized through the PBS of decoder 2. Subsequently, they arrived at port 2 of the upper and lower optical circulators. Fig. 6(a) displays the depolarized spectra (λ_1, λ_3) with a 90° component arriving at the first output port of the PBS in decoder 2 when user 2 sent data bit "1." For these spectra, the central wavelengths of λ_1 and λ_3 were 1543 and 1549 nm, respectively, and the corresponding light intensities were −45.29 and −44.2 dBm. Fig. 6(b) presents the depolarized spectra (λ_2, λ_4) with a 0° component appearing at the second output port of the PBS in decoder 2 when user 2 transmitted data bit "1." For these spectra, the central wavelengths of λ_2 and λ_4 were 1546 and 1552 nm, respectively, and the corresponding light intensities were −39.92 and −38.96 dBm. Fig. 6(c) displays the depolarized spectra (λ_2, λ_4) with a 90° component appearing at the first output port of the PBS in decoder 2 when user 2 sent data bit "0." For these spectra, the central wavelengths of λ_2 and λ_4 were 1546 and 1552 nm, respectively, and the corresponding light intensities were −46.58 and −45.23 dBm. Fig. 6(d) displays the depolarized spectra (λ_1, λ_3) with a 90° component appearing at the first output port of the PBS in FBG decoder 2 when user 2 transmitted data bit "0." For these spectra, the central wavelengths of λ_1 and λ_3 were 1543 and 1549 nm, respectively, and the corresponding light intensities were −36.66 and −36.11 dBm. Therefore, the light output through the free-space channel had an intensity loss of approximately 10–15 dB for the reflected spectra. This loss was due to the effects of atmospheric disturbances and divergence.

The loss difference between the horizontal and vertical paths through the PBS in encoder 2 was estimated to be 5 dB.

The depolarized spectra were then decoded by two series of FBGs, which were coupled in parallel for signal arrival at the input ports of the BPD. Fig. 7(a) displays the decoded spectra $(\lambda_1, \lambda_2, \lambda_3, \lambda_4)$ measured at the output port of the upper coupler in FBG decoder 2 when user 2 had data bit "1." For these spectra, the central wavelengths of $\lambda_1, \lambda_2, \lambda_3$, and λ_4 were 1543, 1546, 1549, and 1552 nm, respectively, and the corresponding light intensities were −45.2, −45.7, −45.46, and −46.43 dBm. Fig. 7(b) illustrates the decoded spectra $(\lambda_1, \lambda_2, \lambda_3, \lambda_4)$ measured at the output port of the lower coupler in FBG decoder 2 when user 2 had data bit "1." For these spectra, the central wavelengths of $\lambda_1, \lambda_2, \lambda_3$, and λ_4 were 1543, 1546, 1549, and 1552 nm, respectively, and all the corresponding light intensities were lower than −53 dBm. Fig. 7(c) displays the decoded spectra $(\lambda_1, \lambda_2, \lambda_3, \lambda_4)$ measured at the output port of the upper coupler in FBG decoder 2 when user 2 had data bit "0." For these spectra, the central wavelengths of $\lambda_1, \lambda_2, \lambda_3$, and λ_4 were 1543, 1546, 1549, and 1552 nm, respectively, and all the corresponding light intensities were lower than −50 dBm. Fig. 7(d) displays the decoded spectra $(\lambda_1, \lambda_2, \lambda_3, \lambda_4)$ measured at the output port of the lower coupler in FBG decoder 2 when user 2 had data bit "0." For these spectra, the central wavelengths of $\lambda_1, \lambda_2, \lambda_3$, and λ_4 were 1543, 1546, 1549, and 1552 nm, respectively, and the corresponding light intensities were −43.94, −45.29, −45, and −46.32 dBm, respectively. The results displayed in Fig. 7 indicate that the performance of the decoded spectra in converting the results into accumulated

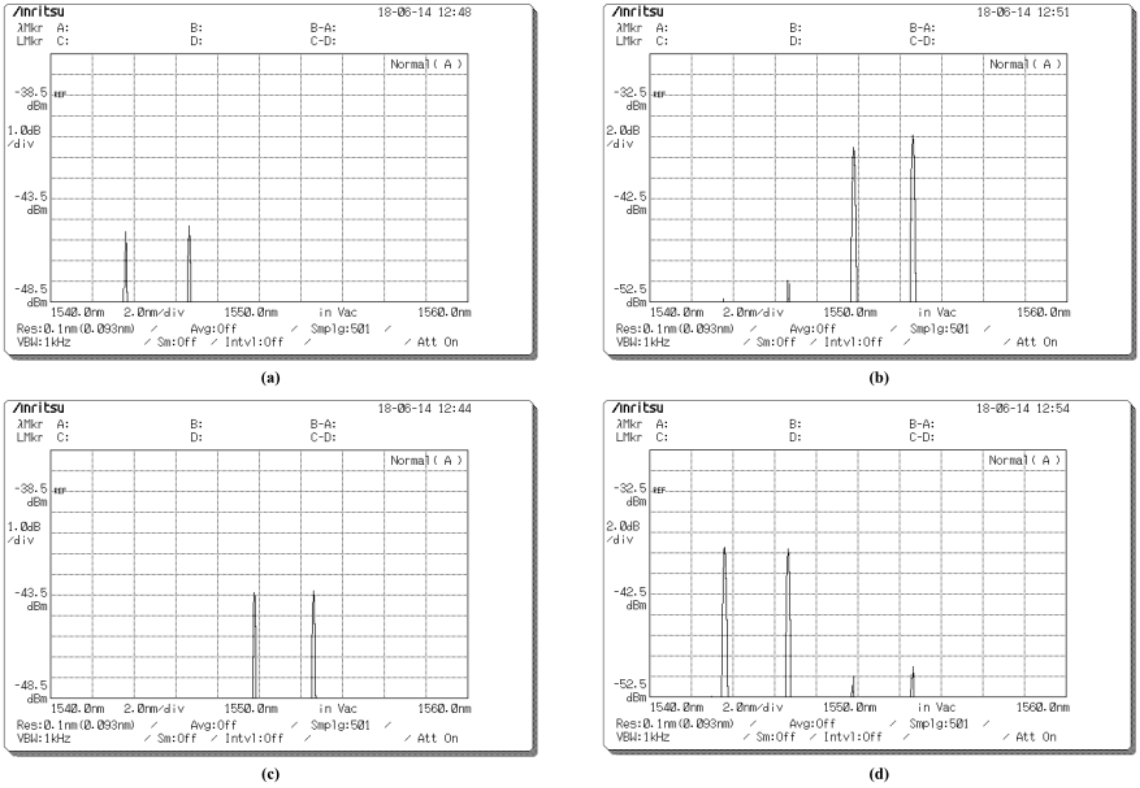

FIGURE 12. Decoded spectra at the input ports of the BPD for different data bits. (a) Optical spectra at the output port of the attenuator in decoder 4 for data bit "1" input to encoder 2. (b) Optical spectra at the output port of the lower coupler in decoder 4 for data bit "1" input to encoder 2. (c) Optical spectra at the output port of the attenuator in decoder 4 for data bit "0" input to encoder 2. (d) Optical spectra at the output port of the lower coupler in decoder 4 for data bit "0" input to encoder 2.

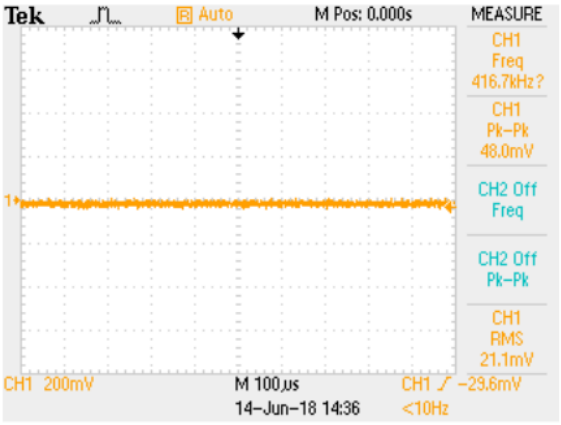

FIGURE 13. Decoding signal for decoder 4 with no signal input into encoder 4 and a 500 Hz signal input into encoder 2.

energy was insufficient, and the background noise at the output of the upper coupler [Fig. 7(c)] revealed some unwanted spectral outputs due to imperfect reflection through FBG decoder 2.

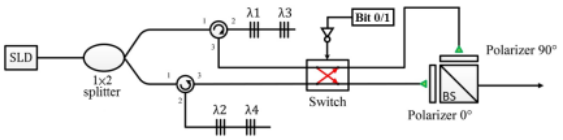

FIGURE 14. Design of the proposed FBG encoder 2 with a Nanona optical switch but without an EDFA.

To test the stability of the entire system, a second experiment was conducted. This experiment involved using an EDFA in encoder 2 to enhance the transmission of light and an attenuator in decoder 2 to mitigate noise (Fig. 8). Fig. 9(a)–(d) displays the decoded spectra at the output ports of the attenuator and lower coupler for system operating with different data bits and using an EDFA and attenuator for FBG codec 2. Fig. 10 displays the decoding results for switching between frequencies during transmission through encoder 2. The BPD was used to convert the decoded spectra into electrical signals. Then, the digital oscilloscope was used to determine the accuracy of data transmission from FBG encoder 2. Fig. 10(a)–(e) displays the decoding results obtained when switching the 2 × 2 optical switch of FBG

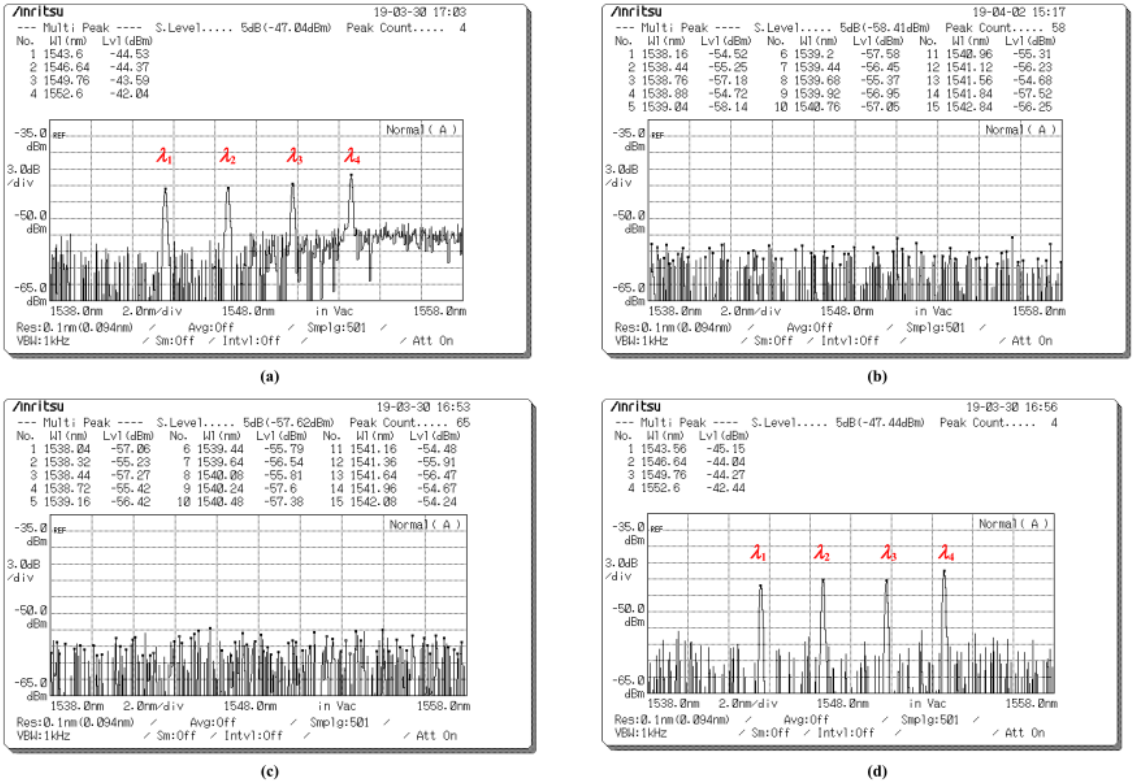

FIGURE 15. Decoded spectra at the input ports of the BPD for encoder 2 obtained using a Nanona ultrafast optical switch and different data bits. (a) Optical spectra at the output port of the attenuator in decoder 2 for data bit "1" input to encoder 2. (b) Optical spectra at the output port of the lower coupler in decoder 2 for data bit "1" input to encoder 2. (c) Optical spectra at the output port of the attenuator in decoder 2 for data bit "0" input to encoder 2. (d) Optical spectra at the output port of the lower coupler in decoder 2 for data bit "0" input to encoder 2.

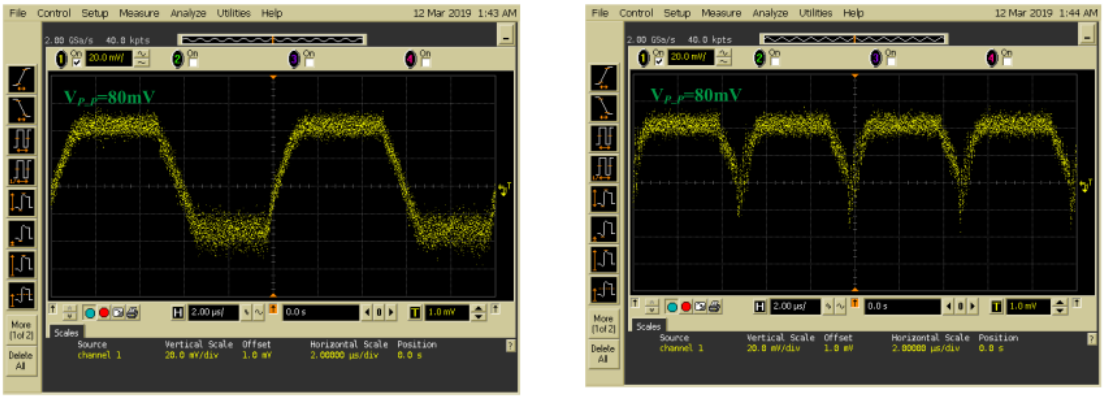

FIGURE 16. Decoding results for decoder 2 with input signal frequencies of (a) 100 and (b) 200 kHz in encoder 2.

encoder 2 to frequencies of 0.1, 0.5, 1, 1.5, and 2 kHz. Fig. 10(e) reveals that when the signal generator transmitted a signal with a frequency of approximately 2 kHz to the optical switch, the decoding result for FBG decoder 2 exhibited severe waveform distortion. This result was obtained because the OSW22-1310E MEMS fiber optical switch kit (Thorlabs, NJ, USA) only supports switching frequencies lower than 2 kHz.

In experiment 3, a switching frequency of 1 kHz was input into FBG encoder 2. Moreover, optical signals from FBG encoder 2 were accessed using FBG decoder 4. Fig. 11 illustrates the architecture of FBG decoder 4.

Fig. 12 illustrates the decoded spectra at the input ports of the BPD using encoder 4 and different data bit inputs to encoder 2. The BPD could convert the decoded spectra into electrical signals. The output results from FBG decoder 4 could then be measured using the digital oscilloscope. Fig. 13 indicates that the designed codec can alleviate the effect of MAI from FBG encoders other than that with the original signal. The alleviation of MAI does not affect the transmitted electrical signal required for access.

In experiment 4, the optical switch of encoder 2 was replaced, and an inverter was used for electrical signal processing. First, a Nanona ultrafast optical switch (Boston Applied Technologies, Inc., MA, USA) was adopted to replace the original fiber optical switch kit and improve the transmission rate of the proposed system. During switching operations, a Nanona optical switch operates differently from an MEMS fiber optical switch. If data bit "0" is input into the Nanona optical switch, it enters parallel operation mode. Conversely, if data bit "1" is input into the Nanona optical switch, it enters cross mode. Therefore, an inverter was used in experiment 4 for converting bits 1 and 0 into electrical signals. The results obtained in experiment 4 were consistent with those obtained with FBG encoders in experiments 1 to 3. Fig. 14 displays the design of the proposed FBG encoder 2 without an EDFA and with a Nanona optical switch.

Fig. 15 displays the decoded spectra at the input ports of the BPD when data bits "1" and "0" were input into FBG encoder 2 by using a Nanona ultrafast optical switch. The digital oscilloscope was used to access the waveform of the signal transmitted by encoder 2, as displayed in Fig. 16. This figure indicates that when the signal generator input a frequency of 100 kHz into the optical switch, the original signal could be reconstructed through the output of FBG decoder 2. However, the results revealed distortion in decoding when a 200 kHz signal was input into FBG encoder 2. This result was obtained because the Nanona optical switch can operate only at frequencies lower than 200 kHz (response time of 5 μs).

The experimental results indicate that the proposed settings and arrangement can effectively mitigate MAI from FBG encoders other than that with the original signal. Moreover, the transmission rate of the proposed FSO system with the bipolar OCDMA scheme could be improved using an ultrafast optical switch. FBGs are used as primary components for constructing the codec; thus, the proposed FSO system is simple and inexpensive.

IV. CONCLUSION

In this study, an FSO communication system using bipolar OCDMA schemes was developed. This system has the advantages of light weight, flexible design, low cost, moderate security level, and resistance to EMI and MAI. The experimental results indicate that the proposed communication system can access the original signal from its encoder without experiencing MAI from other FBG encoders. Interference from other FBG encoders can be avoided with the proposed system, which reduces crosstalk. The experimental results confirm that system stability can be improved by using an EDFA and attenuator. The measurement results for the signal transmission rate revealed the switching limitations of the optical switch. Signals could only be detected at a frequency below 200 kHz. However, the proposed system still presents potential for application, such as in high-maintenance sensor environments and environmental monitoring. With the development of faster optical switches in the future, the proposed FSO system may achieve even higher data rates for multiple users.

REFERENCES

[1] G. D. Lloyd, L. A. Everall, K. Sugden, and I. Bennion, "Resonant cavity time-division-multiplexed fiber Bragg grating sensor interrogator," *IEEE Photon. Technol. Lett.*, vol. 16, no. 10, pp. 2323–2325, Oct. 2004.
[2] Y. Yu, L. Lui, H. Tam, and W. Chung, "Fiber-laser-based wavelength-division multiplexed fiber Bragg grating sensor system," *IEEE Photon. Technol. Lett.*, vol. 13, no. 7, pp. 702–704, Jul. 2001.
[3] L. R. Chen, S. D. Benjamin, P. W. E. Smith, and J. E. Sipe, "Applications of ultrashort pulse propagation in Bragg gratings for wavelength-division multiplexing and code-division multiple access," *IEEE J. Quantum Electron.*, vol. 34, no. 11, pp. 2117–2129, Nov. 1998.
[4] H.-C. Cheng, C.-H. Wu, C.-C. Yang, and Y.-T. Chang, "Wavelength division multiplexing/spectral amplitude coding applications in fiber vibration sensor systems," *IEEE Sensors J.*, vol. 11, no. 10, pp. 2518–2526, Oct. 2011.
[5] S.-P. Tseng, "Fast frequency hopping codes applied to SAC optical CDMA network," *Opt. Fiber Technol.*, vol. 23, pp. 61–65, Jun. 2015.
[6] D. B. Hunter and R. A. Minasian, "Programmable high-speed optical code recognition using fibre Bragg grating arrays," *Electron. Lett.*, vol. 35, no. 5, pp. 412–414, Mar. 1999.
[7] J. A. Salehi, A. M. Weiner, and J. P. Heritage, "Coherent ultrashort light pulse code-division multiple access communication systems," *J. Lightw. Technol.*, vol. 8, no. 3, pp. 478–491, Mar. 1990.
[8] F. Zeng, Q. Wang, and J. Yao, "Sequence-inversion-keyed optical CDMA coding/decoding scheme using an electrooptic phase modulator and fiber Bragg grating arrays," *IEEE J. Sel. Topics Quantum Electron.*, vol. 13, no. 5, pp. 1508–1515, Sep. 2007.
[9] Y.-T. Chang and J.-F. Huang, "Complementary bipolar spectral polarization coding over fiber-grating-based differential photodetectors," *Opt. Eng.*, vol. 45, no. 4, Apr. 2006, Art. no. 045004.

HSU-CHIH CHENG received the B.S. degree from the Electronics Department, National Taiwan University of Science and Technology, in 2000, and the M.S. and Ph.D. degrees in electrical engineering from National Cheng Kung University, Tainan, Taiwan, in 2002 and 2006, respectively. He is currently a Full Professor with the Department of Electro-Optical Engineering, National Formosa University, Yunlin, Taiwan. His major interests lie in DWDM networking devices, optical system design, and optics fiber sensor.

EDDY WIJANTO received the B.S. degree from the Department of Electrical Engineering, Krida Wacana Christian University, Indonesia, in 2005, and the M.S. degree from the Department of Electrical Engineering, Pelita Harapan University, Indonesia, in 2009. He is currently pursuing the Ph.D. degree in Electro-Optical Engineering with National Formosa University, Taiwan. He is also an Assistant Professor with the Department of Electrical Engineering, Krida Wacana Christian University, Indonesia. His major interests are mainly in the areas of wireless and optical communications.

TZU-CHIEH LIEN received the M.S. degree from the Institute of Electro-Optical and Materials Science, National Formosa University, Yunlin, Taiwan. His research interests are mainly in the areas of optics fiber sensors and optical communications.

PO-HAN LAI received the M.S. degree from the Institute of Electro-Optical and Materials Science, National Formosa University, Yunlin, Taiwan. His research interests are mainly in the areas of optics fiber sensors and wireless optical communications.

SHIN-PIN TSENG was born in Taichung, Taiwan, in 1979. He received the B.S. degree in electronic engineering from the National Taipei University of Technology, Taipei, Taiwan, the M.S. degree in electrical engineering from National Cheng Kung University, Tainan, Taiwan, and the Ph.D. degree in communication engineering from National Taiwan University, Taipei, in 2001, 2003, and 2011, respectively. In August 2011, he joined the Electronic Engineering Department, National United University, Miaoli, Taiwan, where he is currently an Associate Professor. His major interests are in code designs and applications for optical code-division multiple-access (OCDMA) communication and in computer communication networks.

EDDY WIJANTO-FILE 5

ORIGINALITY REPORT

4%	3%	3%	1%
SIMILARITY INDEX	INTERNET SOURCES	PUBLICATIONS	STUDENT PAPERS

PRIMARY SOURCES

1	Yan Hua. "SC/APC fiber optic connectors connected and disconnected under high optical power", 2006 Optical Fiber Communication Conference and the National Fiber Optic Engineers Conference, 2006 Publication	1%
2	Submitted to Shri Guru Gobind Singhji Institute of Engineering and Technology Student Paper	<1%
3	orca.cardiff.ac.uk Internet Source	<1%
4	arxiv.org Internet Source	<1%
5	researchonline.federation.edu.au Internet Source	<1%
6	ruor.uottawa.ca Internet Source	<1%
7	Wahhab Abdulrazzaq Abusale, Muhammet Ali Karabulut, Haci Ilhan. "Performance Analysis of Spectral Amplitude Coding Methods in	<1%

Fiber Optical Communication System", Institute of Electrical and Electronics Engineers (IEEE), 2023
Publication

8	eprints.uthm.edu.my Internet Source	<1%
9	www.osapublishing.org Internet Source	<1%
10	academic.oup.com Internet Source	<1%
11	researchonline.gcu.ac.uk Internet Source	<1%

Exclude quotes	On	Exclude matches	< 15 words
Exclude bibliography	On		